Fourier transform infrared spectroscopy analysis of physicochemical changes in UHT milk during accelerated storage

Fourier transform infrared spectroscopy analysis of physicochemical changes in UHT milk during accelerated storage

Manpreet Kaur Grewal[a], Jayani Chandrapala[a], Osaana Donkor[a], Vasso Apostolopoulos[b], Lily Stojanovska[b] and Todor Vasiljevic[a*]

[a]Advanced Food Systems Research Unit and [b]Immunology in Chronic Diseases Program, Centre for Chronic Disease, College of Health and Biomedicine, Victoria University, Melbourne, VIC 8001, Australia

*Corresponding author:

todor.vasiljevic@vu.edu.au

Abstract

Ultra high temperature (UHT) treated milk undergoes substantial physicochemical changes during processing and storage which may lead to sedimentation. Physio-chemical changes leading to sedimentation primarily involve changes in secondary structure of proteins, protein-protein and protein-fat interactions. The study explored feasibility of FTIR to detect these changes. Moreover, accelerated shelf life testing method involving use of high storage temperature was used as an alternative to long realtime analysis to monitor these changes. UHT whole and skim milk were stored at 20, 30, 40 and 50 °C for a period of 28 days. FTIR was able to detect changes leading to increased sedimentation in skim milk and whole milk at higher temperatures (≥40 °C) in a short period of 14 days. Milk samples stored at 40 and 50 °C showed marked changes in the bands corresponding to confirmation of milk lipids and formation of intermolecular β sheet, suggesting protein-lipid interactions and aggregation. Dried sediment contained fat, further evidencing protein-lipid involvement in sedimentation. However, FTIR was not able to detect changes that led to increased sedimentation in skim milk at temperatures lower than 40 °C. A full length study at 20 and 30 °C might enable detection of changes leading to increase in sedimentation at these temperatures. Furthermore, more extensive analysis will be required to establish marker changes in FTIR spectra which could be used for rapid prediction of shelf life of UHT milk.

Keywords: UHT milk, FTIR, structural changes, interactions, aggregation, sedimentation

1. Introduction

UHT treatment of milk (130-140 °C for 3 - 5 seconds) followed by aseptic packaging enables storage of UHT milk at room temperature up to 9 months (Holland, Gupta, Deeth, & Alewood, 2011). Long shelf life at room temperature has made UHT milk an important food product from a nutritional, technological and economical point of view. However, high temperature treatment of milk induces certain chemical and physical changes which may lead to storage instabilities involving formation of proteinaceous sediment at the bottom of the storage container (sedimentation) or a gel throughout the milk (gelation) (Dalgleish, 1992; McMahon, 1996; Ramsey & Swartzel, 1984). Sedimentation or gelation limits shelf life and market potential of UHT milk. Thus, the changes resulting in these instabilities are of concern for the dairy industry.

Physico-chemical changes leading to sedimentation or gelation during storage primarily involve aggregation of milk proteins. Proteins aggregate via crosslinking following different pathways. The most assessed change is mediated by denaturation of whey proteins as a result of UHT treatment (Singh, 1991). Denaturation exposes a free sulfhydryl group of β-lactoglobulin (β-Lg), which is involved in intramolecular and intermolecular thiol-disulfide exchange reactions with other whey proteins and caseins (kappa-casein (κ-CN) and α_{s2}-casein (α_{s2}-CN)) present on the surface of the casein micelles and homogenized fat globules (Sharma & Dalgleish, 1993). Additional crosslinking can also occur via dehydroalanine, deamidated amino acid residues and advanced Maillard products (Holland, et al., 2011).

Aggregation of milk proteins progresses at a slow rate during storage at room temperatures. Studying these changes at room temperature would thus be resource and time consuming. Accelerated shelf life testing methods may be used as an alternative to long realtime analysis as storage temperature accelerates aggregation of milk proteins. However, in our previous study (Grewal, Chandrapala, Donkor, Apostolopoulos, & Vasiljevic, 2016),

protein interactions and especially covalent crosslinking was accelerated at higher storage temperatures but the rate and type of these reactions were very different from those at lower temperatures and was presumably affected by numerous factors due to complex nature of milk. However, acquired knowledge of involvement of individual proteins and kinetics of these changes may assist in identifying structural changes that may be determined by a spectral analysis such as FTIR.

Development and use of proteomic analysis have added information about different types of prospective crosslinking during storage of UHT milk, but these techniques are still limited in elucidating about the related changes in structure and interactions of proteins (Holland, et al., 2011). Furthermore, the sample preparation is fairly laborous accompanied with a complex analysis, all of which require highly trained experts, limiting the application. FTIR spectroscopy could prove to be a simple and fast alternative with minimum sample preparation. FTIR is sensitive to changes in covalent bonding including disulphide linkages, and, non-covalent electrostatic and hydrophobic interactions, which are hallmarks of thermal treatment and subsequent storage. This method has been successfully used to study ageing of pharmaceuticals (Masmoudi, Dréau, Piccerelle, & Kister, 2005) and oil in water emulsions (Whittinghill, Norton, & Proctor, 1999) by determination of changes in molecular structure and interactions, but has not been used in UHT milk. Hence, the study herein aimed to determine the feasibility of FTIR technique to detect physico-chemical changes leading to sedimentation or gelation under accelerated storage temperatures in UHT milk. Besides storage temperature, fat content of milk also influences certain heat-induced modifications in UHT milk (De Koning, Badings, Van der Pol, Kaper, & Vos-Klompmaker, 1990; Pellegrino, 1994) and extent of proteolysis during storage (López-Fandiño, Olano, Corzo, & Ramos, 1993). Thus, the effect of milk fat was also demonstrated on these changes leading to development of storage instabilities.

2. Materials and methods

2.1. Materials

Commercial UHT full cream (whole) (WM) and skim milk (SM) were kindly provided by a local manufacturer (Murray Goulburn Co-operative Co. Ltd., Victoria, Australia). All milk packs originated from the same batch. The packs were produced on the same day using an established process on an indirect tubular processor (SPX Flow Technology, Mulgrave, Australia) with a 9,000 l/hour capacity at 138°C for 6 s. The composition of WM as reported by the manufacturer per litre of milk was 33 g protein, 34 g fat and 53 g sugars, 0.55 g Na and 1.2 g Ca. SM had 34 g protein, 1 g fat and 53 g, 0.55 g Na and 1.2 g Ca per litre of milk. The UHT milk packs were stored at 4 different temperatures, 20, 30, 40 and 50 °C for 28 days in incubators (Thermoline, Scientific Pty Ltd, Smithfield, NSW, Australia). The first 3 temperatures (20, 30, 40 °C) implied storage of UHT milk packs under ambient conditions in cold and relatively hot areas. Storage temperature 50 °C was chosen to accelerate the development of storage instabilities. Milk packs were analyzed on the first day of delivery (day 0), and then at two fortnightly intervals (14 and 28 days) during storage.

2.2. Measurement of sediment

Only sedimentation was observed in samples during storage period. Sedimentation was measured by a centrifugation method as previously described (Boumpa, Tsioulpas, Grandison, & Lewis, 2008) with slight modifications. The milk packs were well shaken and approximately 40 g was accurately weighed in a centrifuge tube and centrifuged at 4000 rpm (2760 g) for 15 min (Beckman Coulter Avanti J-26S XP Centrifuge, CA, USA). The sediment was then oven-dried at 50 °C for 48 hours to a constant weight which was then expressed as the amount of sediment (mg/100g of milk).

2.3. Fourier Transform Infrared Spectroscopy (FTIR)

Three milk packs corresponding to each storage time and temperature were placed at room temperature (20 °C) and equilibrated for six hours. From each pack after shaking the contents, 0.5 ml of sample was pipetted out on Attenuated Total reflectance (ATR) cell. Sample spectra were acquired using PerkinElmer Frontier FTIR spectrometer (PerkinElmer, MA, USA) in the range of 4000-600 cm^{-1} with a resolution on 4 cm^{-1} and by averaging 16 scans of each spectrum. The background spectrum was scanned at the beginning of the measurement with a blank Diamond ATR cell using same instrumental conditions as for sample spectra acquisition. The spectra of three sub samples of each sample were taken by refilling the ATR cell. Spectra of dried sediment corresponding to day 0 and 28^{th} of storage for SM and WM were acquired to estimate composition of sediment.

2.4. Data analysis

The FTIR spectra of all samples were exported to the Unscrambler software (version 9.8; CAMO AS, Trondheim, Norway). The quality of the spectra was checked using their descriptive statistics (Jaiswal, et al., 2015) and visual inspection. This helped to decide suitable pre-processing treatment to remove variation due to baseline shifts, sample concentration on the cell or any factor other than intrinsic variation in the sample. Multivariate analysis technique, Principal Component Analysis (PCA) was then employed to observe classification in UHT milk samples due to storage time and temperature. PCA technique gives an overview of all the information in the data set by generating a new set of fewer coordinate axes called principal components (PCs) with minimum loss of information. PCA was applied before and after different pre-processing treatments to test their effectiveness and detect any outliers.

The sediment dry weight data corresponding to all determinations was analysed using a GLM (Generalized Linear Model) procedure of SAS software (SAS Institute, 1996). The effects of main factors (type of milk, storage time and temperature) and their interactions were analyzed in a split plot in time design at pre-set level of significance $P < 0.05$. The design was replicated 3 times.

3. Results and Discussion

UHT treatment induces structural modifications in milk fat globules and proteins. These modifications lead to change in protein-protein and protein-lipid associations and hence crosslinking during subsequent storage (Corredig & Dalgleish, 1996). This crosslinking may result in formation of aggregates, which remain in milk solution as suspended aggregates until sizeable enough to sediment as insoluble precipitates.

3.1. Sediment formation

Fat content along with storage temperature influenced the extent of sediment formed. In WM, the amount of formed sediment did not increase significantly at and below 30 °C, whereas after 28 days of storage at 40 and 50 °C sediment surged by 28.6 % and 41.3 %, respectively, and was significantly ($P < 0.5$) higher than SM (Table 1). However in SM, besides starting with lower amount of sediment than WM on day 0 ($P < 0.5$), sedimentation increased significantly during 28 days storage irrespective of storage temperature.

Substantial increase in the amount of sediment in WM at elevated temperatures (40 and 50 °C) was accompanied by an increase in appearance of high molecular mass aggregates observed in reducing SDS-PAGE patterns in our previous study (Grewal, et al., 2016). We attributed this primarily to change in protein-lipid interactions as a result of melting of milk fat at 40 °C. Change of physical state of milk lipids results in changed conformation and

packing of constituent phospholipid and triglyceride acyl chains (Boubellouta & Dufour, 2012; Karoui, Mazerolles, & Dufour, 2003), which might have enhanced protein-lipid association in milk at higher storage temperatures resulting in aggregate formation. Presence of lipid absorbance regions in FTIR spectra (3000-2800 cm^{-1}, 1800-1700 cm^{-1}) of sediment in WM (Fig.1B) evidenced that protein-lipid interactions participated in the formation of sediment. Furthermore, increase in intensity of lipid region in dried sediments of WM samples stored at 50 °C compared to those at 20 °C indicated that protein-lipid associations were enhanced by increase in storage temperature. In addition to enhanced protein-lipid interactions, increase in the amount of aggregates in WM at higher temperatures in previous study (Grewal, et al., 2016) was also attributed to protein crosslinking via lipid oxidation products, advanced Maillard products, deamidated and dephosphorylated residues.

Similarly, rise in the amount of sediment in SM at higher temperature could also be associated with protein-lipid association as evidenced by absorbance regions of fat in FTIR spectra of sediment (Fig.1A). However, noticeable changes in the sediment content at storage temperature below 40 °C point at pronounced protein-protein interactions compared to WM. Comparably weak association of denatured whey proteins to the casein micelle surface observed in SM (Garcia-Risco, Ramos, & Lopez-Fandino, 1999) increases their availability for crosslinking reactions taking place in the solution. Whey proteins exhibit greater reactivity than caseins in formation of crosslinks via non-covalent, disulphide and non-disulphide covalent bonding. Apparent fast disappearance of whey proteins in PAGE patterns observed previously (Grewal, et al., 2016) further supports this observation. Enhanced reactivity and disappearance of whey proteins was likely influenced by their denaturation as a consequence of heat treatment resulting in exposure of hydrophobic regions, free thiol groups and preferable amino acid residues like lysine, asparagine, glutamine, which subsequently participated in lactosylation, deamidation and linking via dehydroalanine to caseins

(Andrews, 1975; Donato & Guyomarc'h, 2009; Henle, Schwarzenbolz, & Klostermeyer, 1996; Holland, et al., 2011).

From observations above it appears that changes in protein-lipid and protein-protein interactions during storage govern sediment formation within SM and WM milk samples during storage. Precise identification and prediction of these changes in a shorter time under accelerated conditions could save substantial waiting time to establish sediment formation visually. Therefore, feasibility of FTIR to detect these changes was assessed.

3.2. FTIR

Spectra of SM and WM were predominated by absorption bands of water in regions 3500-3000 cm^{-1} (H-O stretching) and 1730-1600 cm^{-1} (H-O-H bending vibration) (Iñón, Garrigues, & de la Guardia, 2004). This was overcome by subtraction of spectra of water from milk spectra after correcting for baseline offsets. Important spectral regions of milk spectra after water subtraction were 3700-2800 cm^{-1} (Region I), 1800-1700 cm^{-1} (Region II), 1700-1500 cm^{-1} (Region III), 1500-1200 cm^{-1} (Region IV) and 1200-900 cm^{-1} (Region V) (Fig. 2). These regions have been previously attributed to different milk components (Table 2). Multivariate analysis (PCA) was then employed to establish whether FTIR spectra could detect changes that lead to formation of the sediment at different temperatures during storage of SM and WM.

3.3. Principal component analysis

PCA was performed in the regions 4000-600 cm^{-1} (full range) separately for SM and WM samples. In both SM (Fig. 3A1) and WM (Fig. 4A1), first two principal components explained 98% of the variance and classified samples into three separate groups, named A, B and C. Group A comprised of day 28 samples stored at 40 and 50 °C, group B comprised of

day 14 samples stored at 40 and 50 °C and group C constituted samples of day 0 (stored at 20 °C), day 14 and day 28 stored at 20 and 30 °C. Classification of UHT milk samples at and above 40 °C in different groups on the basis of storage time implied that FTIR was able to detect progression of definite changes which resulted in enhanced sedimentation in SM and WM at higher storage temperature (Table 1). However, grouping of SM samples stored at 20 and 30 °C with day 0 samples implied that FTIR was not able to detect such changes at temperatures below 40 °C.

All prominent regions observed in milk spectra (Fig. 2) contributed to the classification of samples into three groups according to the loading plot (Fig. 3A2 & Fig. 4A2). To further investigate specific wavenumbers in these regions and associated changes, PCA was performed independently for regions I-V.

3.3.1. Region I –3700-2800 cm^{-1}

This region registered substantial changes and was able to classify samples into three different groups in both SM (Fig. 3A3) and WM (Fig. 4A3). According to the loading plot (Fig. 3A4 & Fig. 4A4), milk samples were separated along PC1 with high loading for 3594 cm^{-1} and 3193-3194 cm^{-1} (hydrogen bonded O-H stretching), 2926 cm^{-1} (asymmetric stretching modes of CH_2 groups of acyl chains of milk lipids) and 2857 cm^{-1} (symmetric stretching modes of CH_2 groups of acyl chains of triglycerides and phospholipids). The presence of group B (day 14, 40 and 50 °C samples) in-between group C and group A indicated progression of intensity changes of above wavenumbers with storage time.

In samples stored above 40 °C, a shift was observed in a band corresponding to O-H stretch to higher wavenumbers resulting in depression around 3194 cm^{-1} in spectra upon water subtraction (Fig. 5A). Extent of hydrogen bonding (water related) decreases with increase in storage temperature which shifts the O-H stretching frequency to higher

wavenumbers (Choperena & Painter, 2009). On same note, higher negative loading for 3594 cm^{-1} was concomitant with less positive loading at 3194 cm^{-1} in group A samples compared to group C.

Group A also experienced decrease in loadings for 2926 and 2857 cm^{-1} with storage time (Fig 4A4). The shift in these wavenumbers has been used previously to study phase transition of phospholipids (sol to gel state transition) with increase in temperature (Dufour, et al., 2000). Milk fat melts around 40 °C which in turn results in prominent structural changes and interactions of milk lipids (Dufour, et al., 2000). These changes in turn lead to protein-lipid interactions indicated by reduction in the absorbance intensities (Fig 5A) and lower loading for group A as compared to group C samples (Fig. 4A4).Even though, the peaks corresponding to wavenumbers 2926 and 2857 cm^{-1} were not visible in loading plot of region I in SM (Fig. 3A4), the fat B region (3000-2800cm^{-1}) was independently able to classify samples into three groups A, B and C. Therefore, enhanced protein-lipid associations may also account for greater sedimentation observed at higher storage temperatures in both SM and WM (Table 1).

3.3.2 *Region II 1800-1700 cm^{-1}*

Region II, attributed to milk fat A, classified storage samples into three groups in both SM (Fig. 3A5) and WM (Fig. 4A5). In WM, according to loading plot (Fig. 4A6), principal component 2 separated group B samples from group C whereas Group A samples were further separated from group B samples by principal component 1. Samples stored above 40 °C after 14 days had higher loading mainly for 1754, 1749 cm^{-1}, 1736 cm^{-1}, 1719 cm^{-1}, 1714 cm^{-1} and 1704 cm^{-1}. Loading plot of principal component 1 revealed further increase in above mentioned wavenumbers for samples stored above 40 °C after 28 days. In SM, group A, B and C were separated along principal component 2. The loading plot of PC 2 in SM

(Fig.3A6) indicated higher loading for group A samples for same wavenumbers as in WM however with lower absorbance intensities due to lower fat content.

The flattening of peak around 1754 cm^{-1} (Fig 5B) corresponds to changes in C=O stretching vibrations of ester linkage pertaining to triglycerides (Karoui, et al., 2003). Changes in physical state of lipids at and above 40 °C also affected carbonyl stretching vibrations of ester linkage of triglycerides. Changes in stretching of ester linkage might be also due to protein-lipid association via its carbonyl groups (Surewicz, Moscarello, & Mantsch, 1987). Higher loading around 1720 cm^{-1} had been associated previously with presence of hydrogen bonded carbonyl groups of esters (Dufour & Riaublanc, 1997). In addition, wavenumbers 1720 and 1715 cm^{-1} had also been assigned to C=O stretching vibration of aldehydes and ketones respectively. Advanced Maillard products (AMP) and lipid oxidation products were noted previously as participants in crosslinking of proteins at higher temperatures due to presence of aldehyde and ketone functional groups (Hm-Major, 1997). Thus, higher loading for 1720 and 1715 cm^{-1} for group A and B implies an elevated content of AMP and oxidation products in samples stored at higher temperatures with storage time, which in addition to enhanced lipid-protein associations could further influence the rate of sedimentation at higher temperatures.

3.3.3 Region III Protein (Amide I and Amide II) 1700-1500 cm^{-1}

Classification of storage samples into groups A, B and C by this region in both SM (Fig. 3A7) and WM (Fig.4A7) implies changes in protein secondary structure, protein-protein and protein-lipid interactions at elevated storage temperature (Karoui, et al., 2003; Mendelsohn, Mao, & Flach, 2010; Sankaram & Marsh, 1993). The region III has two main parts namely amide I (1700-1600 cm^{-1}) corresponding to C=O stretching vibrations of the peptide bonds and amide II (1600-1500 cm^{-1}) attributed to C-N stretching vibrations in

combination with N-H bending (Kher, Udabage, McKinnon, McNaughton, & Augustin, 2007).

In WM, group A and B samples separated from group C samples due to increase in loading principally for 1696, 1686, 1653, 1647, 1634, 1628 and 1622 cm^{-1} (amide I), 1578, 1571, 1558, 1539, 1531, 1522, 1515 and 1506 cm^{-1} (amide II) (Fig. 4A8). However in SM, samples group A and B separated due to increase in almost similar wavenumbers apart from a shift in 1628 cm^{-1} and amide II wavenumbers (Fig. 3A8). This shift was also observed in spectra of this region for SM (Fig. 5A3).

Increase in loading at 1697, 1686 and 1618 cm^{-1} with storage at higher temperature suggests formation of aggregates consisting of intermolecular β sheet (Mendelsohn & Flach, 2002; Mendelsohn, et al., 2010; Ngarize, Herman, Adams, & Howell, 2004). In addition, surge in loading around 1620-1618 cm^{-1} had also been attributed to disruption of intramolecular hydrogen bonds within a secondary structure, leading to formation of new stronger intermolecular hydrogen bonds (Ngarize, et al., 2004). However, unlike previously reported (Murphy, Fenelon, Roos, & Hogan, 2014), increase in intermolecular β sheet (1686 and 1618 cm^{-1}) in the current study was not followed with concomitant decline in α-helix (1653 cm^{-1}) and intramolecular β sheet structure (1630−1627 cm^{-1}). It appeared that though there was an enhancement in intermolecular interactions leading to the aggregation, it was not at expense of intramolecular interactions. Otherwise, it can also be argued that amide I vibration could not distinguish clearly between α-helical and random-coil structures (Anderle & Mendelsohn, 1987), and thus, increase at 1653 cm^{-1} might also correspond to increase in random coil structure. Moreover, increase in random coil (1645 cm^{-1}) and turns (1676 cm^{-1}) could also be associated with increased participation of caseins in formation of aggregates. In addition to increase in protein-protein interactions at higher storage temperature, protein-lipid

interactions, initiated by changed physical state, had also been reported to induce the formation of intermolecular hydrogen bonded β sheets resulting in protein aggregation (Sankaram & Marsh, 1993).

Schiff base intermediates formed during the course of Maillard browning reactions have been reported to absorb at 1647 cm^{-1}(Murphy, et al., 2014). Increase in intensity at 1647 cm^{-1} in both SM and WM in Group A and B samples suggests that lactosylation could be one of the confounding factors (Fig. 3A8 &4A8). Interestingly, absorbance at 1647 cm^{-1} was higher for SM than WM supporting higher rate of Maillard reaction in former as suggested in our previous study (Grewal, et al., 2016).

In amide II region, a band around 1575 cm^{-1} (Fig. 3A8 & 4A8) has been used previously as a marker for start of acidification in cheese ripening process with formation of lactates (Mazerolles, et al., 2001). In the current study, a band appearing at 1577 cm^{-1} may be caused by a decline in pH with storage (data not shown). Peaks at 1569 cm^{-1} arise from the $-COO^-$ asymmetric stretching vibration of Asp and Glu residues, and increase in its loading might be due to deamidation of amino acid residues observed during storage at elevated temperatures in UHT milk. Deamidated residues are also known to serve as protein crosslinkers and hence may play a role in formation of aggregates (Holland, et al., 2011). Higher loading for 1569 cm^{-1} in group A samples in WM compared to those in SM (Fig.3A8 & Fig.4A8) also confirms our previous observation (Grewal, et al., 2016) that deamidation was a contributing factor in formation of aggregates in WM. Loading peak at 1515 cm^{-1} indicates changes in ring-stretching vibration of the tyrosine residues which could be further related to their oxidation and crosslinking. Loadings for wavenumbers in 1578-1555, 1555-1543 and 1542-1525 cm^{-1} region had also been attributed to changes in amount of β turns, alpha helices/ loops and β sheets, respectively (Curley, Kumosinski, Unruh, & Farrell, 1998).

3.3.4 Region IV Protein (Amide III) 1500-1200 cm^{-1}

Amide III spectral region also corresponds to secondary structure of proteins. Although, having relatively weak signals in contrast to most commonly used amide I region (1700–1600 cm^{-1}), amide III does not suffer from several limitations including a strong interference from water vibrational band, relatively unstructured spectral contour and overlap of revolved bands correspondingly to various secondary structures (Fu, Deoliveira, Trumble, Sarkar, & Singh, 1994). The peaks in this region correspond to N-H bending and C-N stretching vibrations (Jaiswal, et al., 2015) and also to CH_2 scissoring of acyl chains of lipids (Mendelsohn, et al., 2010).

The region classified samples into three groups A, B and C only in WM samples (Fig. 4A9). In SM, only group A was separated from the combined cluster consisting of group B and C (Fig.3A9). This could imply that milk fat and its content play an important role storage stability of UHT milk. Highest loading for the secondary structure frequency windows (unordered, 1288–1256 cm^{-1}; and β-sheets, 1255–1224 cm^{-1}) for group A samples in both SM and WM (Fig.3A10 & Fig. 4A10) further stressed on formation of β sheet and greater participation of caseins in protein aggregation and consequently sedimentation. In spite of lower loading for group A samples for α-helix (1328–1289 cm^{-1}), it still could not be certainly said that determined whether increase in β-sheet conformation related to protein aggregation was concomitant with previously reported decline in α-helical structure (Murphy, et al., 2014; QI, et al., 1997). Furthermore, presence of a large number of observed bands in the loading plot obscured finding a particular difference between SM and WM. Furthermore, slight variations in helical geometry, symmetry, or interactions result in changed amide III frequencies, so that simple correlations between narrow frequency ranges and secondary structures may not be applicable for this mode (Anderle & Mendelsohn, 1987).

However, lower loadings for CH_2 scissoring of acyl chains of lipids (1500-1400 cm^{-1}). (Fig. 3A10 & 4A10) in group A samples could be assigned to enhanced association between protein and lipids as a result of changed physical state of lipids at higher temperatures. Furthermore, due to diminished amount of fat in SM, this may be a major factor substantiating the classification of samples into 2 groups only and not distinctively into 3 groups like in WM.

3.3.5 Region V (1200-900 cm^{-1})

This region was able to classify samples into two groups (A and combined B & C) only in WM (Fig 4A11). In SM it was not able separate samples into different groups. However, when PCA was applied for combined Region IV and V in SM, it clearly separated samples into three groups A, B and C (Fig 3A11).

Loading plot in WM indicated high loading for 1176, 1148, 1143, 1115, 1058, 1046, 1014 and 997 cm^{-1} which separated group A samples from the remaining two groups (Fig. 4A12). In this region, a peak around 1159 cm^{-1} has been previously associated with C-O vibrations of milk fat (Zhou, et al., 2006). As discussed earlier, the milk fat was sensitive to high storage temperatures governing the extent of protein-lipid associations which resulted in greater sedimentation for WM. Low fat content might have reduced the signal which could have resulted in no separation in SM when only 1200-900 cm^{-1} was considered.

The area between 800 and 1250 cm^{-1} embodies characteristic peaks of various C–O vibrations in carbohydrates, mainly lactose (Zhou, et al., 2006). It was expected from earlier observations and suggestions that due to higher amount of AMP in SM, the chemical changes accompanying the Maillard reaction would lead to several changes in its mid-infrared spectrum. However, inability of region to classify samples in SM implied that changes as a result of Maillard reactions were not intense enough to be detected by FTIR. Maillard

reactions principally involve the consumption of NH_2 functional groups typically from lysine with the appearance of other new functional groups such as the Amadori compound (C=O), Schiff base (C=N), and pyrazines (C-N). Even though lactose is present in a high concentration, it is only depleted by a small margin via the Maillard reactions due to absence of sufficient reactive amino groups. Lysine, one of the predominant reacting amino function in proteins because of the reactivity and availability of its -amino group, comprises less than 0.25% by mass of SM. Subsequently, the concentration of the reaction products would be relatively low. In addition, reactants and products would share many functional groups, thus any changes may not be detectable (Turner, et al., 2002).

Bands around 995 and 987 cm^{-1} suggested changes in stretching vibrations of $-PO_3^{2-}$ moiety of the serine-phosphate residue. The appearance of the two bands had been earlier related to release of CCP particles from the phosphate residues by pressure and its dissociation into Ca^{2+} and $HPO4^{2-}$, resulting in an increased negative charge of the casein molecules (Gebhardt, Takeda, Kulozik, & Doster, 2011). In our study, this may be related to heat- induced elimination of phosphate from phosphoserine residues in caseins producing dehydroalanine, which subsequently reacts with amino group of lysine residues, imidazole group of histidine or thiol group of cysteine resulting in intra or intermolecular lysinoalanine, histidinoalanine or lanthionine crosslinks, respectively (Holland, et al., 2011). It may also imply dissociation of CCP and increase in ionic calcium which was also observed during storage (data not shown).

4. Conclusions

FTIR was able to detect changes in samples stored at and above 40 °C in 14 days. This suggested that it may take even less than 14 days to detect significant changes using FTIR spectroscopy when using accelerated storage temperatures. In addition, it appeared that

changes in structure and interaction of milk lipids propelled the separation of samples according to storage temperatures and time in both SM and WM. Next major contribution to the classification of storage samples was from changes in protein structure and interactions. Increase in sediment was correlated with increase in intermolecular β sheet. In addition changes in proteins, changes in carbohydrates due Maillard reaction were present but were less intense may be due to the duration of storage study. In addition, inability to detect changes in SM at 20 and 30 °C which resulted in increased sediment might require a longer duration study. Furthermore, longer study will also enable to detect more specific markers used to predict the shelf life of UHT milk.

5. Acknowledgement

This work is supported by the Department of Business and Innovation of the Victorian Government, through its Victoria India Doctoral Scholarship Program (managed by the Australia India Institute). The first author also acknowledges her employer Indian Council of Agricultural Research for granting study leave to pursue Ph.D.

References

Anderle, G., & Mendelsohn, R. (1987). Thermal denaturation of globular proteins. Fourier transform-infrared studies of the amide III spectral region. *Biophysical Journal, 52*, 69-74.

Andrews, A. (1975). Properties of aseptically packed ultra-high-temperature milk: III. Formation of polymerized protein during storage at various temperatures. *Journal of Dairy Research, 42*, 89-99.

Boubellouta, T., & Dufour, É. (2012). Cheese-matrix characteristics during heating and cheese melting temperature prediction by synchronous fluorescence and mid-infrared spectroscopies. *Food and Bioprocess Technology, 5*, 273-284.

Boumpa, T., Tsioulpas, A., Grandison, A. S., & Lewis, M. J. (2008). Effects of phosphates and citrates on sediment formation in UHT goats' milk. *Journal of Dairy Research, 75*, 160-166.

Choperena, A., & Painter, P. (2009). Hydrogen Bonding in Polymers: Effect of Temperature on the OH Stretching Bands of Poly(vinylphenol). *Macromolecules, 42*, 6159-6165.

Corredig, M., & Dalgleish, D. G. (1996). Effect of different heat treatments on the strong binding interactions between whey proteins and milk fat globules in whole milk. *Journal of Dairy Research, 63*, 441-449.

Curley, D. M., Kumosinski, T. F., Unruh, J. J., & Farrell, H. M. (1998). Changes in the secondary structure of bovine casein by Fourier transform infrared spectroscopy: Effects of calcium and temperature. *Journal of Dairy Science, 81*, 3154-3162.

Dalgleish, D. G. (1992). Sedimentation of Casein Micelles During the Storage of Ultra-High Temperature Milk Products—a Calculation. *Journal of Dairy Science, 75*, 371-379.

De Koning, P., Badings, H., Van der Pol, J., Kaper, J., & Vos-Klompmaker, E. (1990). Effect of heat treatment and fat content on the properties of UHT-milk. *Voedingsmiddelentechnologie (Netherlands)*.

Donato, L., & Guyomarc'h, F. (2009). Formation and properties of the whey protein/$\ kappa $-casein complexes in heated skim milk–A review. *Dairy Science and Technology, 89*, 3-29.

Dufour, E., & Riaublanc, A. (1997). Potentiality of spectroscopic methods for the characterisation of dairy products. II. Mid infrared study of the melting temperature of cream triacylglycerols and of the solid fat content in cream. *Lait, 77*, 671-681.

Dufour, E., Mazerolles, G., Devaux, M. F., Duboz, G., Duployer, M. H., & Mouhous Riou, N. (2000). Phase transition of triglycerides during semi-hard cheese ripening. *International Dairy Journal, 10*, 81-93.

Fu, F.-N., Deoliveira, D. B., Trumble, W. R., Sarkar, H. K., & Singh, B. R. (1994). Secondary structure estimation of proteins using the amide III region of Fourier transform infrared spectroscopy: application to analyze calcium-binding-induced structural changes in calsequestrin. *Applied spectroscopy, 48*, 1432-1441.

Garcia-Risco, M. R., Ramos, M., & Lopez-Fandino, R. (1999). Proteolysis, protein distribution and stability of UHT milk during storage at room temperature. *Journal of the Science of Food and Agriculture, 79*, 1171-1178.

Gebhardt, R., Takeda, N., Kulozik, U., & Doster, W. (2011). Structure and stabilizing interactions of casein micelles probed by high-pressure light scattering and FTIR. *The Journal of Physical Chemistry B, 115*, 2349-2359.

Grewal, M. K., Chandrapala, J., Donkor, O., Apostolopoulos, V., & Vasiljevic, T. (2016). Electrophoretic characterization of protein interactions suggesting limited feasibility of accelerated shelf life testing of UHT milk. *Journal of Dairy Science, Under review*.

Henle, T., Schwarzenbolz, U., & Klostermeyer, H. (1996). Irreversibles crosslinking of casein during storage of UHT-treated skim milk. In *Heat treatments and alternative methods. IDF Symposium, Vienna (Austria), 6-8 Sep 1995*: International Dairy Federation.

Hm-Major, S. (1997). *Investigation of the chemistry of 1-hydroxyacetone by Fourier transform infrared spectroscopy.* McGill University.

Holland, J. W., Gupta, R., Deeth, H. C., & Alewood, P. F. (2011). Proteomic Analysis of Temperature-Dependent Changes in Stored UHT Milk. *Journal of Agricultural and Food Chemistry, 59*, 1837-1846.

Iñón, F. A., Garrigues, S., & de la Guardia, M. (2004). Nutritional parameters of commercially available milk samples by FTIR and chemometric techniques. *Analytica Chimica Acta, 513*, 401-412.

Jaiswal, P., Jha, S. N., Borah, A., Gautam, A., Grewal, M. K., & Jindal, G. (2015). Detection and quantification of soymilk in cow–buffalo milk using Attenuated Total Reflectance Fourier Transform Infrared spectroscopy (ATR–FTIR). *Food Chemistry, 168*, 41-47.

Karoui, R., Mazerolles, G., & Dufour, É. (2003). Spectroscopic techniques coupled with chemometric tools for structure and texture determinations in dairy products. *International Dairy Journal, 13*, 607-620.

Kher, A., Udabage, P., McKinnon, I., McNaughton, D., & Augustin, M. A. (2007). FTIR investigation of spray-dried milk protein concentrate powders. *Vibrational spectroscopy, 44*, 375-381.

López-Fandiño, R., Olano, A., Corzo, N., & Ramos, M. (1993). Proteolysis during storage of UHT milk: differences between whole and skim milk. *Journal of Dairy Research, 60*, 339-347.

Masmoudi, H., Dréau, Y. L., Piccerelle, P., & Kister, J. (2005). The evaluation of cosmetic and pharmaceutical emulsions aging process using classical techniques and a new method: FTIR. *International Journal of Pharmaceutics, 289*, 117-131.

Mazerolles, G., Devaux, M.-F., Duboz, G., Duployer, M.-H., Riou, N. M., & Dufour, É. (2001). Infrared and fluorescence spectroscopy for monitoring protein structure and interaction changes during cheese ripening. *Le Lait, 81*, 509-527.

McMahon, D. J. (1996). Age-gelation of UHT milk: changes that occur during storage, their effect on shelf life and the mechanism by which age-gelation occurs. In *Heat treatments and alternative methods. IDF Symposium, Vienna (Austria), 6-8 Sep 1995*: International Dairy Federation.

Mendelsohn, R., & Flach, C. R. (2002). Infrared reflection-absorption spectroscopy of lipids, peptides, and proteins in aqueous monolayers. *Current Topics in Membranes, 52*, 57-88.

Mendelsohn, R., Mao, G., & Flach, C. R. (2010). Infrared reflection–absorption spectroscopy: Principles and applications to lipid–protein interaction in Langmuir films. *Biochimica et Biophysica Acta (BBA) - Biomembranes, 1798*, 788-800.

Murphy, E. G., Fenelon, M. A., Roos, Y. H., & Hogan, S. A. (2014). Decoupling macronutrient interactions during heating of model infant milk formulas. *Journal of Agricultural and Food Chemistry, 62*, 10585-10593.

Ngarize, S., Herman, H., Adams, A., & Howell, N. (2004). Comparison of Changes in the Secondary Structure of Unheated, Heated, and High-Pressure-Treated β-Lactoglobulin and Ovalbumin Proteins Using Fourier Transform Raman Spectroscopy and Self-Deconvolution. *Journal of Agricultural and Food Chemistry, 52*, 6470-6477.

Pellegrino, L. (1994). Influence of fat content on some heat-induced changes in milk and cream. *Nederlands melk en Zuiveltijdschrift, 48*, 71-80.

QI, X. L., Carl, H., MCNULTY, D., CLARKE, D. T., BROWNLOW, S., & JONES, G. R. (1997). Effect of temperature on the secondary structure of β-lactoglobulin at pH 6.7, as determined by CD and IR spectroscopy: a test of the molten globule hypothesis. *Biochemical Journal, 324*, 341-346.

Ramsey, J. A., & Swartzel, K. R. (1984). Effect of Ultra High Temperature Processing and Storage Conditions on Rates of Sedimentation and Fat Separation of Aseptically Packaged Milk. *Journal of Food Science, 49*, 257-262.

Sankaram, M. B., & Marsh, D. (1993). Protein-lipid interactions with peripheral membrane proteins. *New Comprehensive Biochemistry, 25*, 127-162.

Sharma, S. K., & Dalgleish, D. G. (1993). Interactions between milk serum proteins and synthetic fat globule membrane during heating of homogenized whole milk. *Journal of Agricultural and Food Chemistry, 41*, 1407-1412.

Singh, H. (1991). Modification of food proteins by covalent crosslinking. *Trends Food Sci Technol, 2*, 196-200.

Surewicz, W. K., Moscarello, M. A., & Mantsch, H. H. (1987). Fourier transform infrared spectroscopic investigation of the interaction between myelin basic protein and dimyristoylphosphatidylglycerol bilayers. *Biochemistry, 26*, 3881-3886.

Turner, J. A., Sivasundaram, L. R., Ottenhof, M.-A., Farhat, I. A., Linforth, R. S. T., & Taylor, A. J. (2002). Monitoring Chemical and Physical Changes during Thermal Flavor Generation. *Journal of Agricultural and Food Chemistry, 50*, 5406-5411.

Whittinghill, J. M., Norton, J., & Proctor, A. (1999). A fourier transform infrared spectroscopy study of the effect of temperature on soy lecithin-stabilized emulsions. *Journal of the American Oil Chemists' Society, 76*, 1393-1398.

Zhou, Q., Sun, S.-Q., Yu, L., Xu, C.-H., Noda, I., & Zhang, X.-R. (2006). Sequential changes
520 of main components in different kinds of milk powders using two-dimensional infrared correlation analysis. *Journal of Molecular Structure, 799*, 77-84.

Figure Legends

Fig.1. FTIR of dried sediment of UHT on day 0 (0d) and 28th day (28d) stored at 20 °C and 50 °C (A) skim milk (SM) and (B) whole milk (WM).

Fig.2 (a) FTIR spectra of UHT whole milk on day 0 of storage in the range 4000-600 cm^{-1} with different regions of interest (I-V) marked on it

Fig.3 Principal component scores and loading plots of spectra acquired at 0, 14 and 28th day of UHT skim milk packs stored at 20 °C, 30 °C, 40 °C and 50 °C for spectral range (A 1-2) 4000-600 cm^{-1}, (A 3-4) region I - 3700-2800 cm^{-1}, (A 5-6) region II- 1800-1700 cm^{-1}, (A 7-8) region III-1700-1500cm^{-1}, (A 9-10) region IV 1500-1200 cm^{-1} and (A 11-12) region V 1500-900 cm^{-1}. Group A comprising of 28th day samples stored at 40 °C and 50 °C, Group B comprising of 14th day samples stored at 40 and 50 °C and Group C constituting 0 day, 14th day (20 °C and 30 °C) and 28th day (20 °C and 30 °C).

Fig.4 Principal component scores and loading plots of spectra acquired at 0, 14 and 28th day of UHT whole milk packs stored at 20 °C, 30 °C, 40 °C and 50 °C for spectral range (A 1-2) 4000-600 cm^{-1}, (A 3-4) region I - 3700-2800 cm^{-1}, (A 5-6) region II- 1800-1700 cm^{-1}, (A 7-8) region III-1700-1500cm^{-1}, (A 9-10) region IV 1500-1200 cm^{-1} and (A 11-12)region V 1200-900 cm^{-1}. Group A comprising of 28th day samples stored at 40 and 50 °C, Group B comprising of 14th day samples stored at 40 °C and 50 °C and Group C constituting 0 day, 14th day (20 °C and 30 °C) and 28th day (20 °C and 30 °C).

Fig.5 FTIR spectra of UHT whole milk in the region 3700-2800 cm^{-1} (A1) and 1800-1700 cm^{-1} (A2) and UHT skim milk in the region 1700-1500 cm^{-1}.

Table 1.
Effect of type of milk (skim or whole milk), time and temperature on amount of sediment (insoluble precipitates) formed in UHT

	Sediment, mg/100g of milk							
	Skim milk				Whole milk			
	Storage time, day							
Temperature (° C)	0	7	21	28	0	7	21	28
20	52.5^{a}	68.8^{bA}	90.1^{cA}	96.8^{deA}	93.6^{ecd}	105.4^{deA}	99.9^{cdeA}	105.6^{cdeA}
30	-	63.1^{bA}	95.0^{cA}	99.4^{dA}	-	99.4^{ecdA}	92.0^{ecdA}	104.3^{ecdA}
40	-	67.1^{bA}	93.1^{cA}	92.4^{dA}	-	108.9^{eA}	101.2^{ecdA}	120.4^{fB}
50	-	69.4^{bA}	106.4^{cB}	101.7^{cA}	-	122.5^{dB}	119.7^{dB}	132.3^{eB}
SEM	4.32							

* Means in the same row that do not share the same small letters differ ($P < 0.05$)

** Means in the same column that do not share the same capital letters differ ($P < 0.05$)

Table 2.

Milk components attributed to different regions of FTIR spectra

IR region (cm^{-1})	Milk component	Reference
3000-2800	Milk lipids (Fat B)	Iñón, et al. (2004)
1800-1700	Milk lipids (Fat A)	Iñón, et al. (2004)
1700-1600	Milk proteins-amide I	Karoui, et al. (2003); Murphy, et al. (2014)
1600-1500	Milk proteins-amide II	Karoui, et al. (2003)
1500-1200	Milk proteins-amide III, interactions between different milk components (Fingerprint region)	Anderle and Mendelsohn (1987); (Kher, et al., 2007)
1200-900	Milk minerals; milk fat, lactose (Fingerprint region	Zhou, et al. (2006); Gebhardt, et al. (2011); Kher, et al. (2007)

Fig. 1.

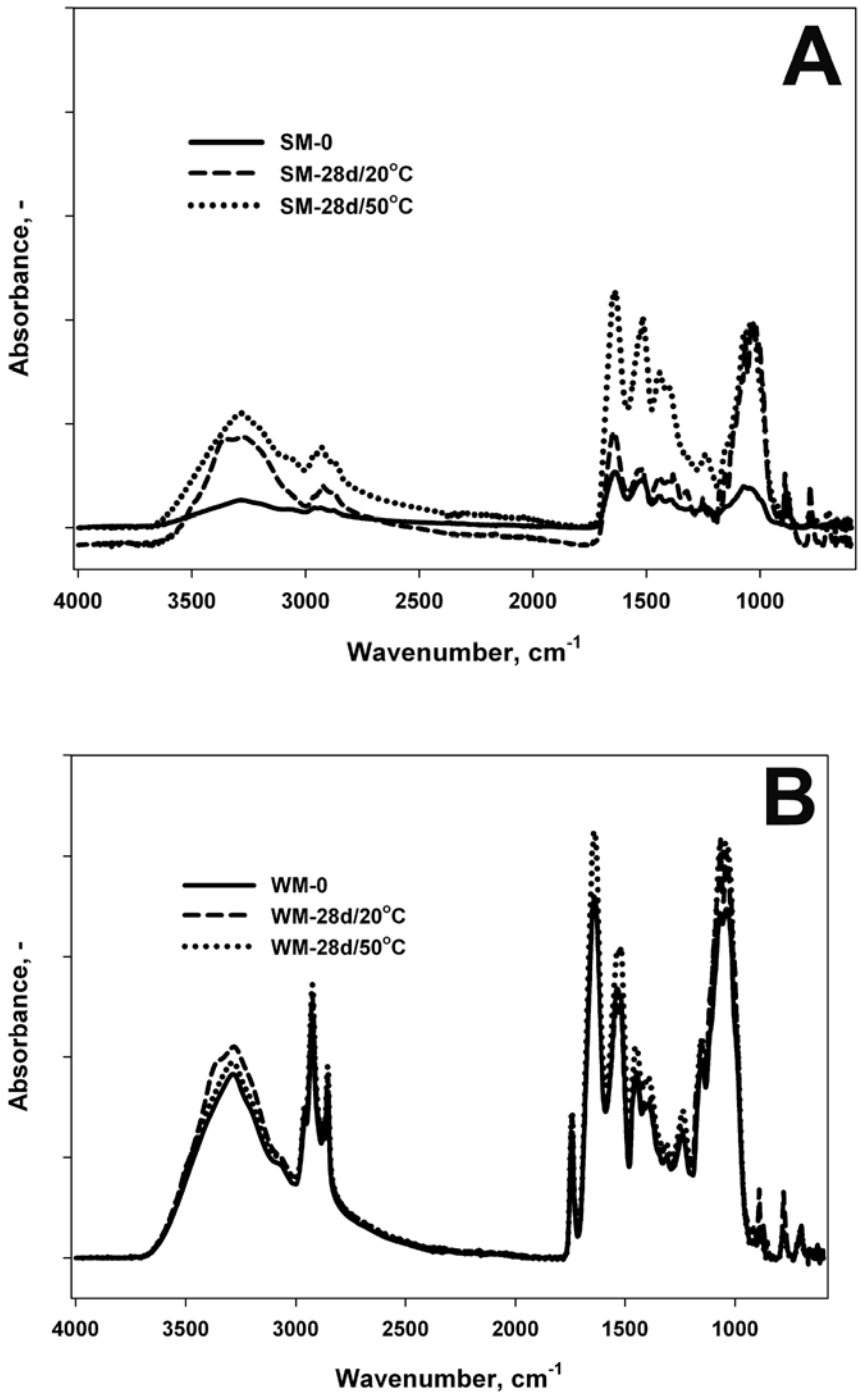
A
SM-0
SM-28d/20°C
SM-28d/50°C
Absorbance, -
4000
3500
3000
2500
2000
1500
1000
Wavenumber, cm-1
B
WM-0
WM-28d/20°C
WM-28d/50°C
Absorbance, -
4000
3500
3000
2500
2000
1500
1000
Wavenumber, cm-1

Fig. 2.

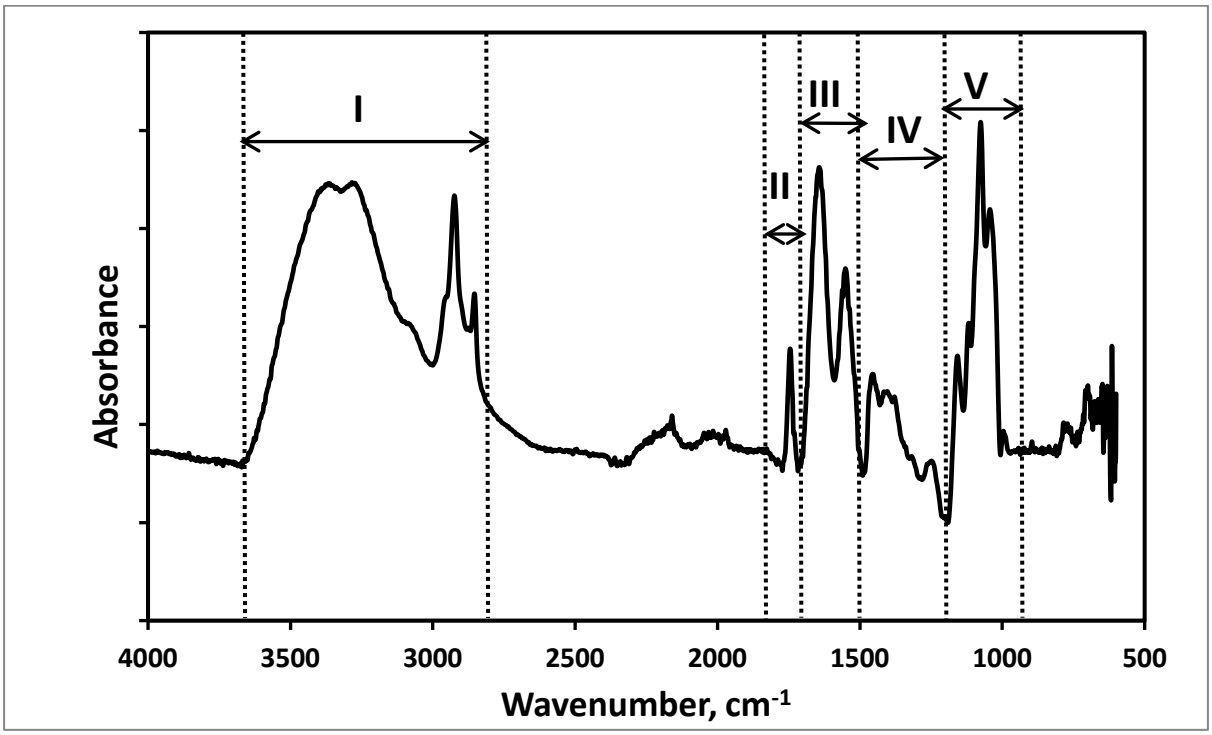
I
II
III
IV
V
Absorbance
4000
3500
3000
2500
2000
1500
1000
500
Wavenumber, cm-1

Fig 3. SM

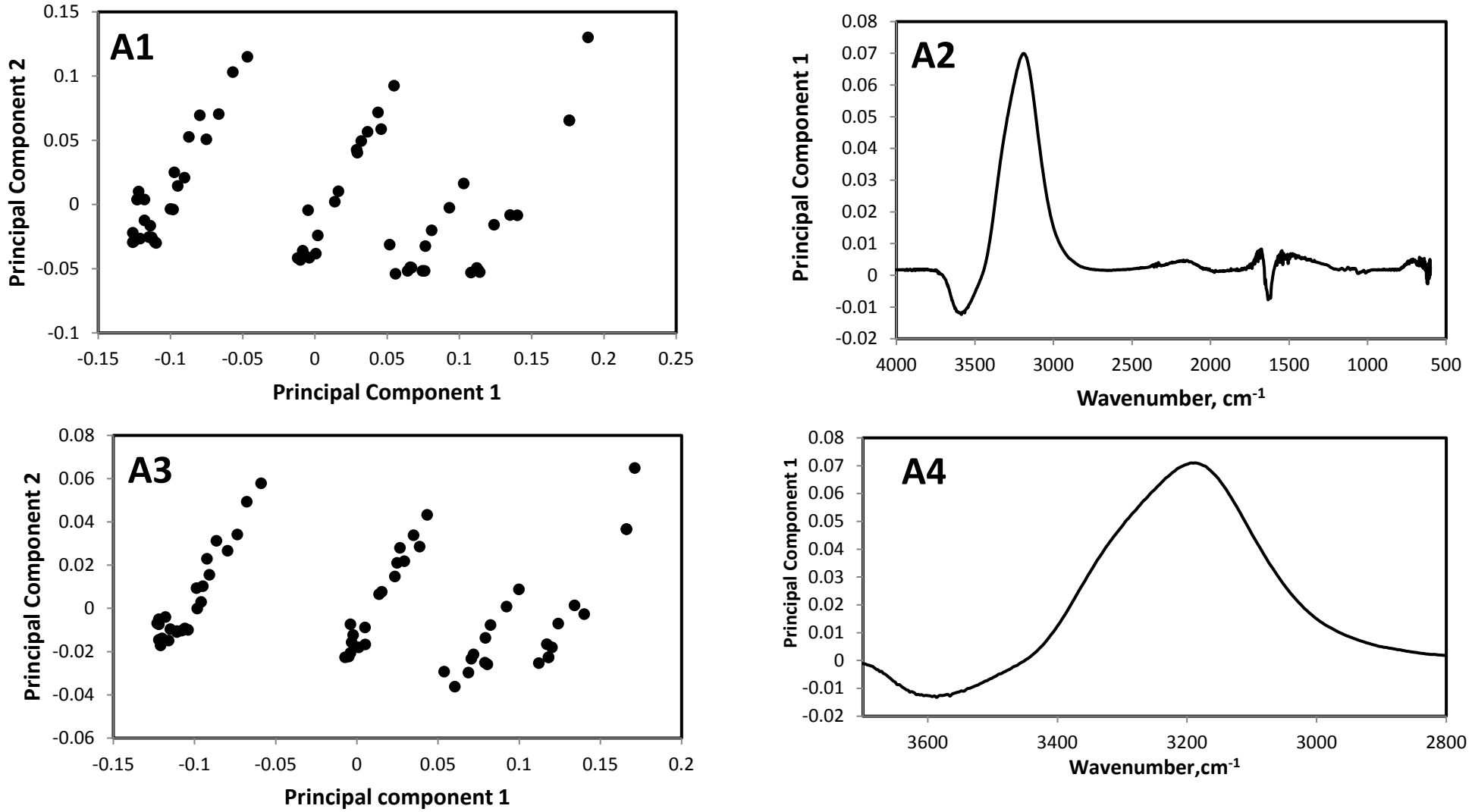
A1
Principal Component 2
Principal Component 1
A2
Principal Component 1
Wavenumber, cm-1
A3
Principal Component 2
Principal component 1
A4
Principal Component 1
Wavenumber,cm-1

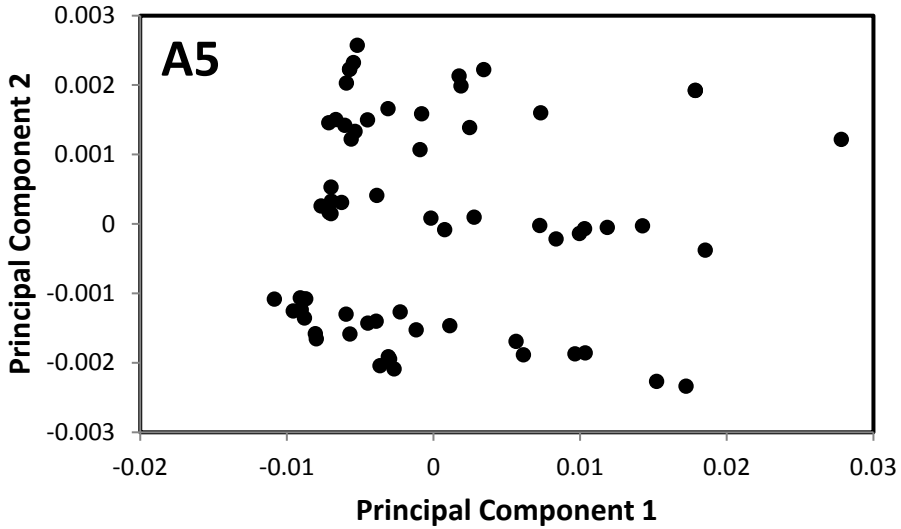
A5
Principal Component 2
Principal Component 1
0.003
0.002
0.001
0
-0.001
-0.002
-0.003
-0.02
-0.01
0
0.01
0.02
0.03

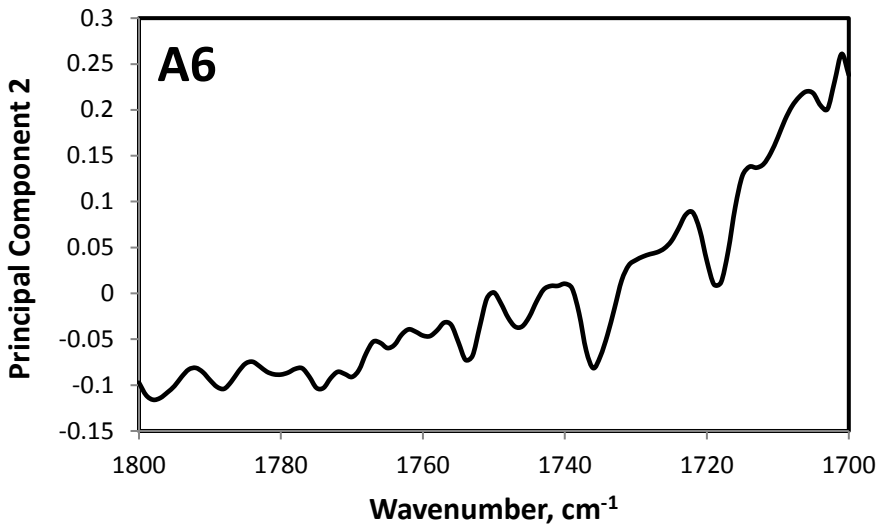
A6
Principal Component 2
Wavenumber, cm-1
0.3
0.25
0.2
0.15
0.1
0.05
0
-0.05
-0.1
-0.15
1800
1780
1760
1740
1720
1700

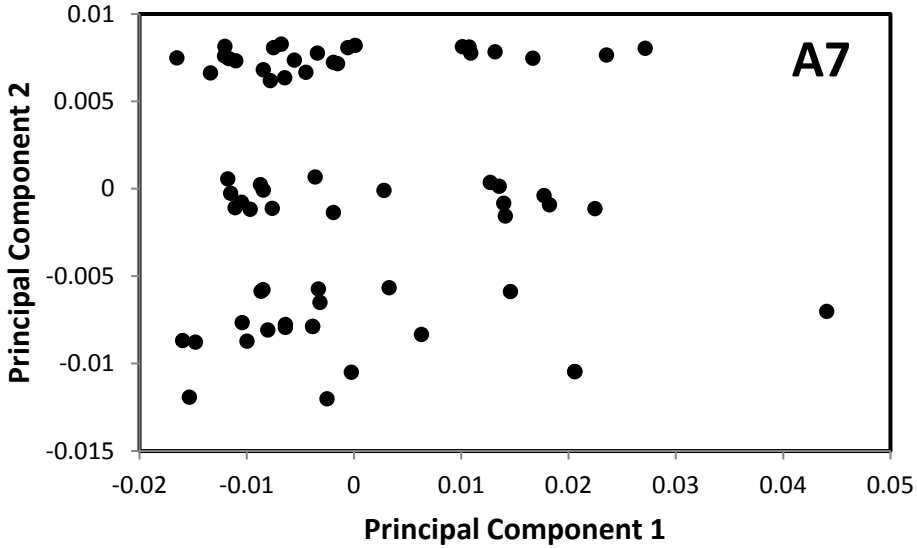
A7
Principal Component 2
Principal Component 1
0.01
0.005
0
-0.005
-0.01
-0.015
-0.02
-0.01
0
0.01
0.02
0.03
0.04
0.05

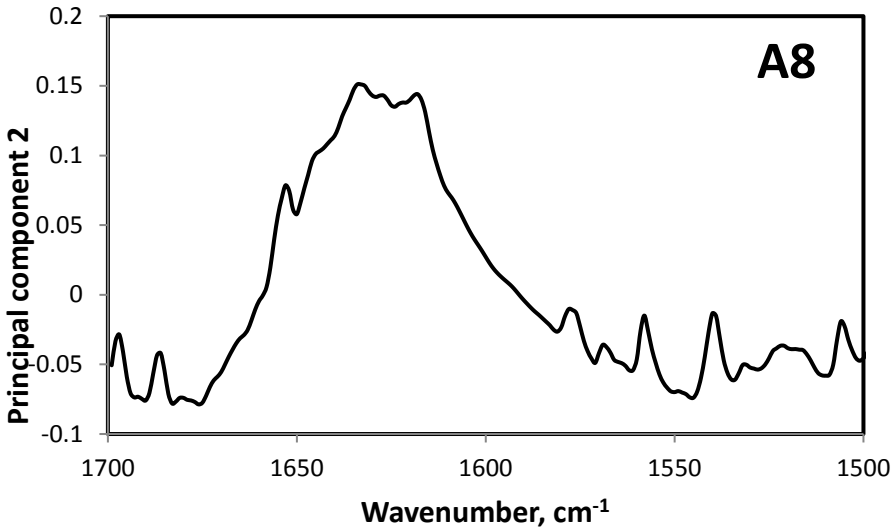
A8
Principal component 2
Wavenumber, cm-1
0.2
0.15
0.1
0.05
0
-0.05
-0.1
1700
1650
1600
1550
1500

526

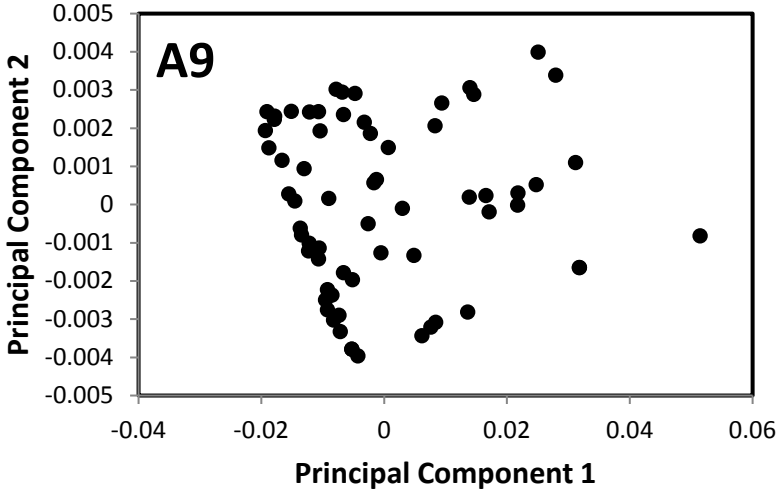
A9
Principal Component 2
Principal Component 1
0.005
0.004
0.003
0.002
0.001
0
-0.001
-0.002
-0.003
-0.004
-0.005
-0.04
-0.02
0
0.02
0.04
0.06

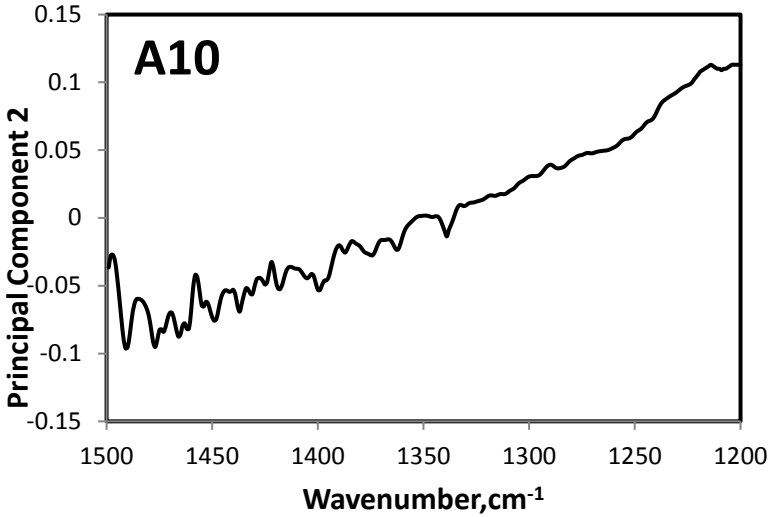
A10
Principal Component 2
Wavenumber,cm-1
0.15
0.1
0.05
0
-0.05
-0.1
-0.15
1500
1450
1400
1350
1300
1250
1200

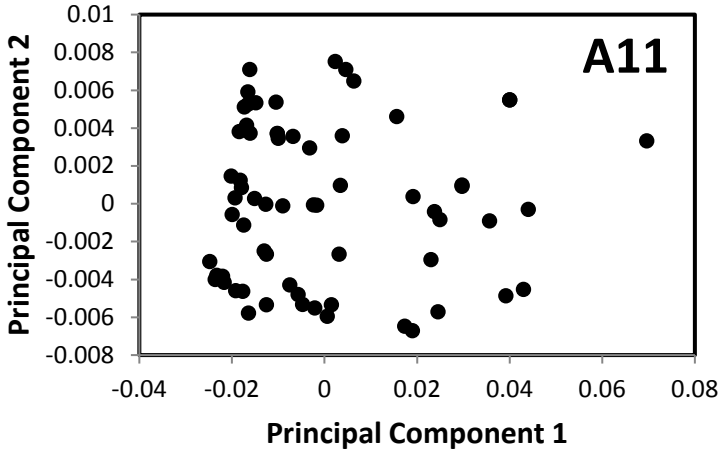
A11
Principal Component 2
Principal Component 1
0.01
0.008
0.006
0.004
0.002
0
-0.002
-0.004
-0.006
-0.008
-0.04
-0.02
0
0.02
0.04
0.06
0.08

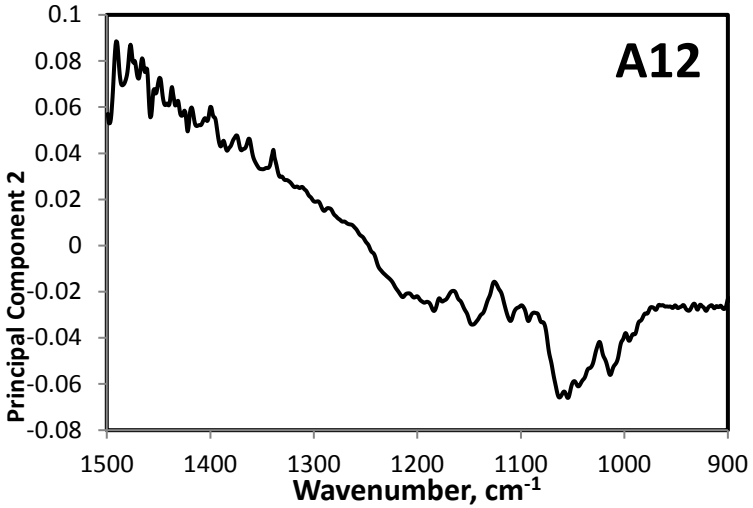
A12
Principal Component 2
Wavenumber, cm-1
0.1
0.08
0.06
0.04
0.02
0
-0.02
-0.04
-0.06
-0.08
1500
1400
1300
1200
1100
1000
900

Fig. 4 WM

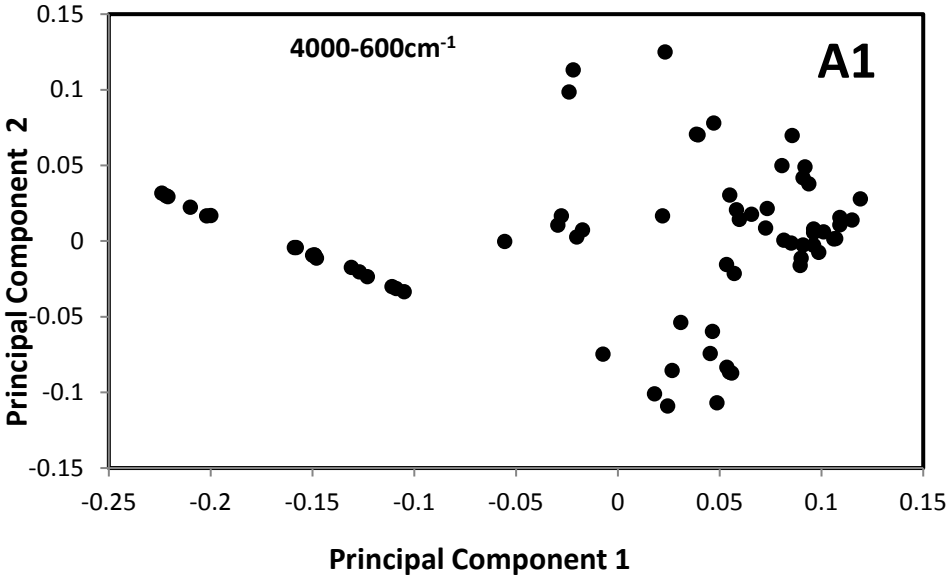
4000-600cm-1
A1
Principal Component 2
Principal Component 1
0.15
0.1
0.05
0
-0.05
-0.1
-0.15
-0.25
-0.2
-0.15
-0.1
-0.05
0
0.05
0.1
0.15

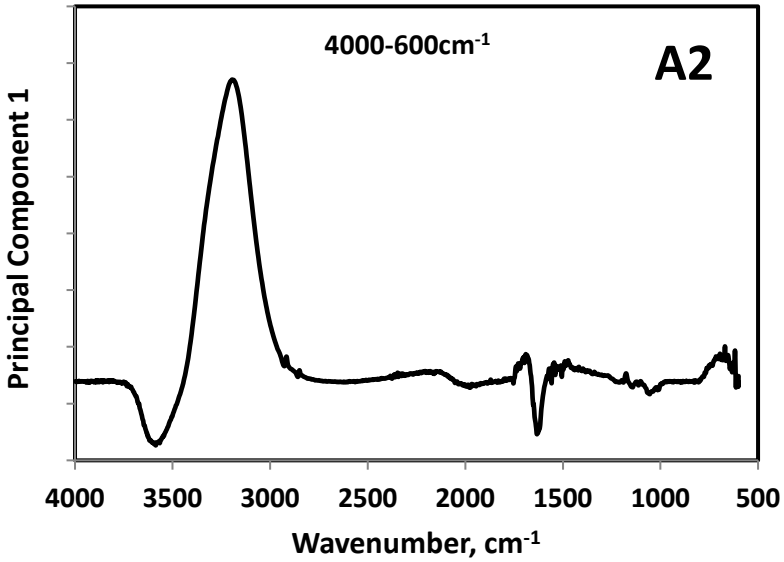
4000-600cm-1
A2
Principal Component 1
Wavenumber, cm-1
4000
3500
3000
2500
2000
1500
1000
500

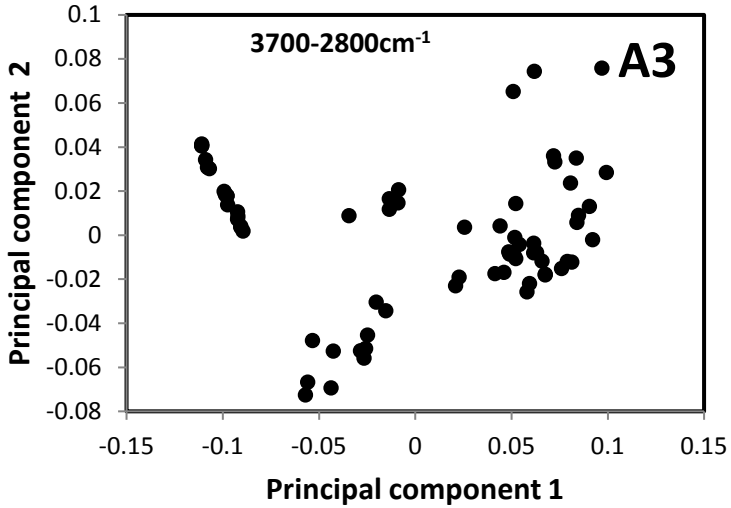
3700-2800cm-1
A3
Principal component 2
Principal component 1
0.1
0.08
0.06
0.04
0.02
0
-0.02
-0.04
-0.06
-0.08
-0.15
-0.1
-0.05
0
0.05
0.1
0.15

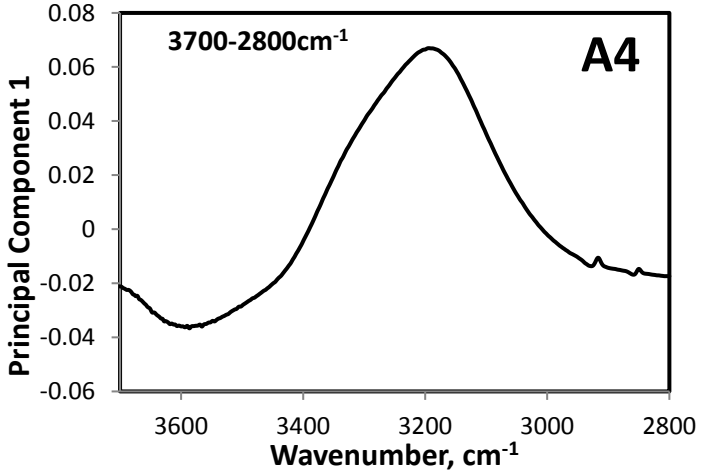
3700-2800cm-1
A4
Principal Component 1
Wavenumber, cm-1
0.08
0.06
0.04
0.02
0
-0.02
-0.04
-0.06
3600
3400
3200
3000
2800

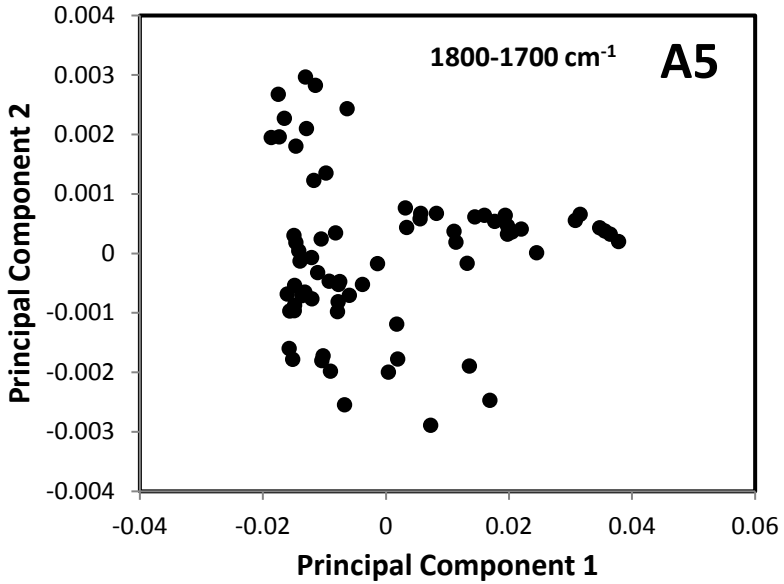
A5
1800-1700 cm-1
Principal Component 2
Principal Component 1
0.004
0.003
0.002
0.001
0
-0.001
-0.002
-0.003
-0.004
-0.04
-0.02
0
0.02
0.04
0.06

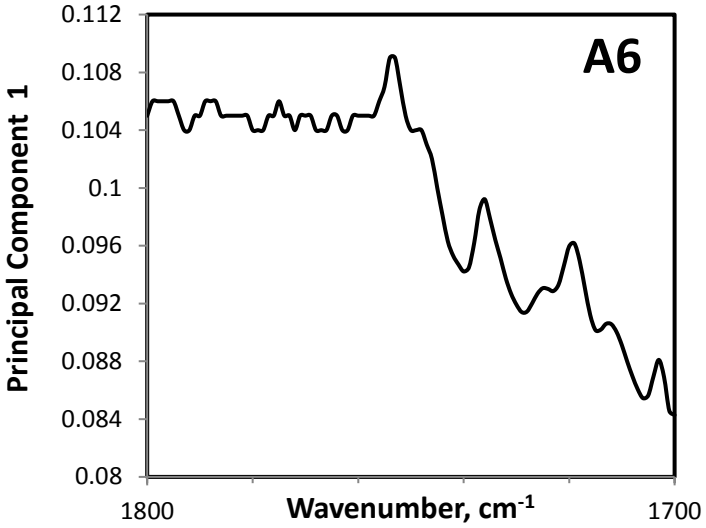
A6
Principal Component 1
Wavenumber, cm-1
0.112
0.108
0.104
0.1
0.096
0.092
0.088
0.084
0.08
1800
1700

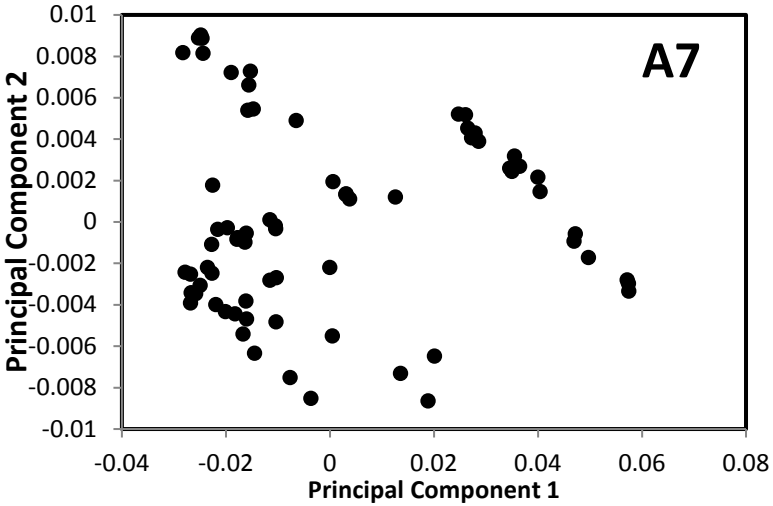
A7
Principal Component 2
Principal Component 1
0.01
0.008
0.006
0.004
0.002
0
-0.002
-0.004
-0.006
-0.008
-0.01
-0.04
-0.02
0
0.02
0.04
0.06
0.08

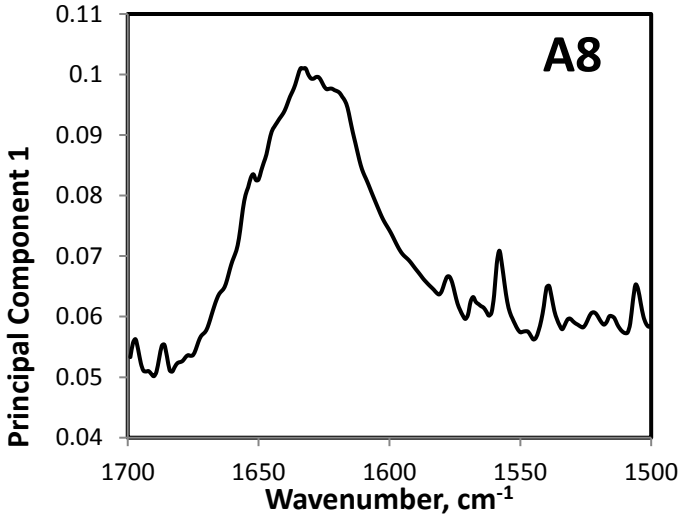
A8
Principal Component 1
Wavenumber, cm-1
0.11
0.1
0.09
0.08
0.07
0.06
0.05
0.04
1700
1650
1600
1550
1500

529

530

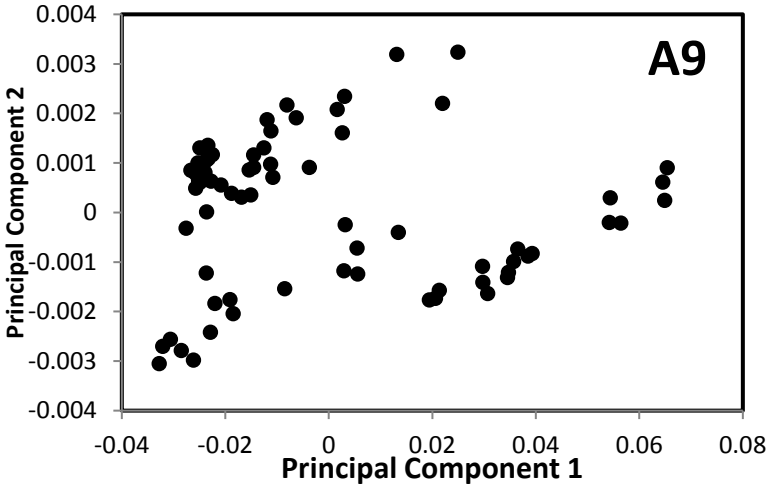
A9
Principal Component 2
Principal Component 1
0.004
0.003
0.002
0.001
0
-0.001
-0.002
-0.003
-0.004
-0.04
-0.02
0
0.02
0.04
0.06
0.08

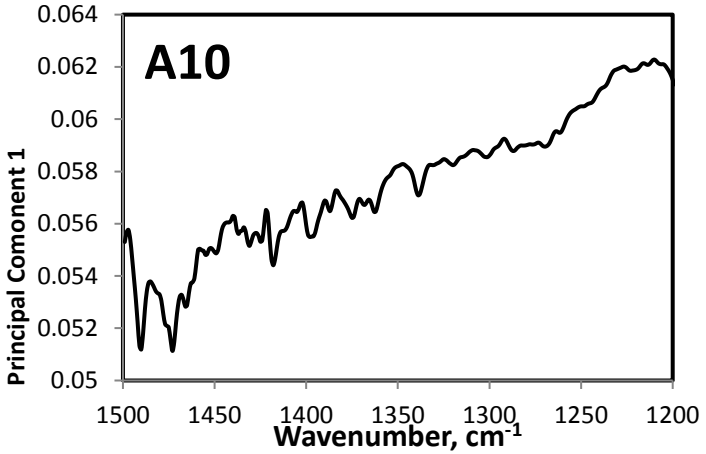
A10
Principal Comonent 1
Wavenumber, cm-1
0.064
0.062
0.06
0.058
0.056
0.054
0.052
0.05
1500
1450
1400
1350
1300
1250
1200

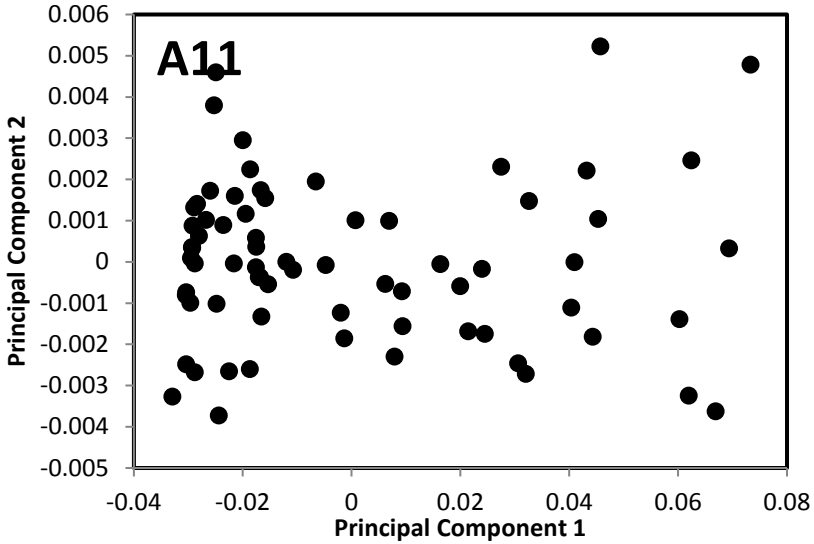
A11
Principal Component 2
Principal Component 1
0.006
0.005
0.004
0.003
0.002
0.001
0
-0.001
-0.002
-0.003
-0.004
-0.005
-0.04
-0.02
0
0.02
0.04
0.06
0.08

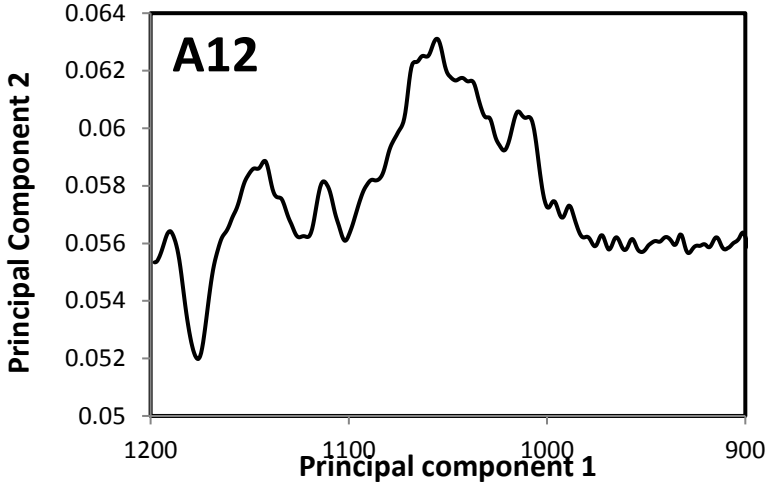
A12
Principal Component 2
Principal component 1
0.064
0.062
0.06
0.058
0.056
0.054
0.052
0.05
1200
1100
1000
900

531 **Fig.5**

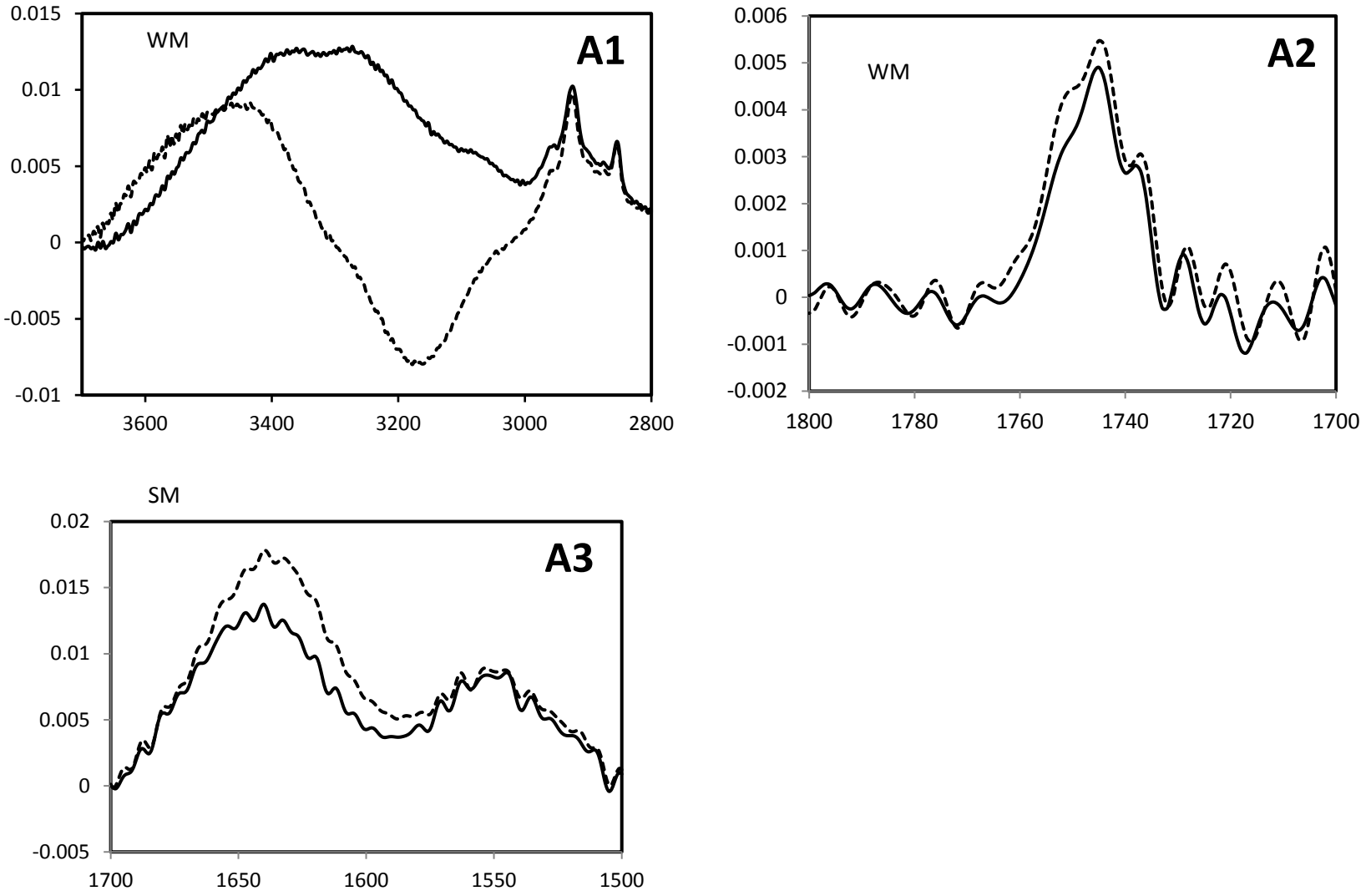
WM
A1
0.015
0.01
0.005
0
-0.005
-0.01
3600
3400
3200
3000
2800
WM
A2
0.006
0.005
0.004
0.003
0.002
0.001
0
-0.001
-0.002
1800
1780
1760
1740
1720
1700
SM
A3
0.02
0.015
0.01
0.005
0
-0.005
1700
1650
1600
1550
1500

532